Low-temperature antiferromagnetic moments at the 4a site in $Ce_3Pd_{20}Ge_6$

2000 J. Phys.: Condens. Matter 12 9441

(http://iopscience.iop.org/0953-8984/12/45/307)

J. Phys.: Condens. Matter **12** (2000) 9441–9451. Printed in the UK PII: S0953-8984(00)14398-X

Low-temperature antiferromagnetic moments at the 4a site in $Ce_3Pd_{20}Ge_6$

A Dönni†*, T Herrmannsdörfer‡, P Fischer‡, L Keller‡, F Fauth§#, K A McEwen‖, T Goto¶ and T Komatsubara+

† Department of Physics, Niigata University, Niigata 950-2181, Japan
‡ Laboratory for Neutron Scattering, ETH Zürich and Paul Scherrer Institute, CH-5232 Villigen PSI, Switzerland
§ Institute Laue–Langevin, F-38042 Grenoble, France
‖ University College London, Department of Physics and Astronomy, London WC1E 6BT, UK
¶ Graduate School of Science and Technology, Niigata University, Niigata 950-2181, Japan
+ Centre of Low Temperature Physics, Tohoku University, Sendai 980-8578, Japan

E-mail: donni@sc.niigata-u.ac.jp (A Dönni)

Received 1 June 2000

Abstract. We have performed powder neutron diffraction experiments to examine the magnetic ordering in $Ce_3Pd_{20}Ge_6$, which exhibits ferroquadrupolar ordering at $T_{Q1} \approx 1.2$ K and antiferromagnetic ordering at $T_{N2} = 0.75$ K. In the series of isostructural cubic rare-earth (R) compounds $R_3Pd_{20}X_6$ (X = Si, Ge; space group $Fm\bar{3}m$), it is common that at the Néel temperature T_{N1} the magnetic moments at the 8c site (simple cubic sublattice) order in an antiferromagnetic sequence with propagation vector $\boldsymbol{k}_1 = [1, 1, 1]$ and at T_{N2} the magnetic moments at the 4a site (face-centred cubic sublattice) order with a propagation vector $\boldsymbol{k}_2 = [0, 0, 1]$. In $Ce_3Pd_{20}Ge_6$ the Néel temperature T_{N1} is replaced by T_{Q1} and at the 8c site a possible ordered cerium moment is found to be reduced to an undetectable small value down to the lowest measured temperature $T = 0.05$ K. In contrast, at the 4a site the cerium moments order below T_{N2} with the expected antiferromagnetic structure. The moments align perpendicular to the propagation vector $\boldsymbol{k}_2 = [0, 0, 1]$ with a saturation value $\mu_2(4a) = (1.1 \pm 0.1)\ \mu_B$/Ce that is reasonably large for the crystal field ground-state quartet Γ_8. Our results provide indirect experimental evidence that only the quadrupolar moments of cerium at the 8c site are involved in the phase transition at T_{Q1}.

1. Introduction

Besides their magnetic dipole moment, rare-earth elements with incomplete 4f electron shells are known to also possess higher-order moments like quadrupole and octupole ones. For most rare-earth compounds the pair interactions between 4f electrons located at neighbouring sites give rise to the ordering of the 4f dipole moments in a long-range magnetic structure below a Néel temperature T_N or a Curie temperature T_C. Accordingly, the quadrupole moments also usually have non-zero values in the magnetically ordered state, but this is induced by the dipole ordering. Of special interest are the rare cases where the quadrupole moments order on their own in a phase transition at T_Q. For Ce-based compounds, quadrupolar ordering has been observed in CeB_6 [1, 2], CeAg [3] and most recently in $Ce_3Pd_{20}Ge_6$ [4, 5]. CeB_6 shows

* Author to whom any correspondence should be addressed. Telephone: (+81)-25-262 6136; fax: (+81)-25-263 3961.
# Present address: Swiss Light Source Project, Paul Scherrer Institute, CH-5232 Villigen PSI, Switzerland.

0953-8984/00/459441+11$30.00

antiferroquadrupolar ordering at T_Q = 3.3 K and antiferromagnetic ordering at T_N = 2.3 K. CeAg exhibits ferroquadrupolar ordering at T_Q = 15.9 K and ferromagnetic ordering at T_C = 5.2 K. For $Ce_3Pd_{20}Ge_6$, ferroquadrupolar order at $T_Q \approx 1.2$ K and antiferromagnetic order at T_N = 0.75 K have been reported. In all of these compounds the $J = 5/2$ multiplet of the Ce^{3+} ions is split by the crystalline-electric-field interactions of cubic symmetry into a Γ_8 quartet ground state and a Γ_7 doublet excited state. For the Γ_8 quartet the irreducible representation of the multipolar 4f moments consists of 15 independent order parameters [6]: three dipole moments (first-rank J-tensors: J_x, J_y, J_z), five quadrupole moments (second-rank J-tensors: O_2^0, O_2^2, O_{xy}, O_{yz}, O_{zx}) and seven octupole moments (third-rank J-tensors: T_{xyz}, T_x^α, T_y^α, T_z^α, T_x^β, T_y^β, T_z^β). The order parameter of the phase transition at T_Q has been suggested to be a linear combination of O_{xy}, O_{yz} and O_{zx} in CeB_6 [2], O_2^0 in CeAg [3] and O_2^0 or O_2^2 in $Ce_3Pd_{20}Ge_6$ [5, 7].

$Ce_3Pd_{20}Ge_6$ is a member of the ternary intermetallic compound series $R_3Pd_{20}Ge_6$ (R = only light rare-earth elements) and $R_3Pd_{20}Si_6$ (R = all rare-earth elements). The cubic crystal structure (space group $Fm\bar{3}m$) of these 3–20–6 systems is an ordered derivative of the $Cr_{23}C_6$-type structure [8] and the magnetic rare-earth atoms occupy the two crystallographic sites 4a (face-centred cubic sublattice) and 8c (simple cubic sublattice). 3–20–6 systems with magnetic crystal-field ground states usually exhibit two antiferromagnetic phase transitions at T_{N1} and T_{N2}. The magnetic structures of several 3–20–6 compounds have already been examined by neutron diffraction experiments: $Tb_3Pd_{20}Si_6$ (T_{N1} = 10.2 K, T_{N2} = 4.1 K [9]), $Dy_3Pd_{20}Si_6$ ($T_{N1} \approx 5.8$ K, $T_{N2} \approx 1.8$ K [10]), $Nd_3Pd_{20}Ge_6$ (T_{N1} = 1.75 K, T_{N2} = 0.58 K [11–13]), $Nd_3Pd_{20}Si_6$ (T_{N1} = 2.4 K, T_{N2} = 0.7 K [14]) and $Ho_3Pd_{20}Si_6$ (T_{N1} = 2.0 K, T_{N2} = 0.5 K, for $T \geqslant 1.5$ K [15]). Common to all these systems are magnetic structures with the same propagation vectors: below T_{N1} the rare-earth moments at the 8c sites order in an antiferromagnetic sequence with a propagation vector $\boldsymbol{k}_1 = [1, 1, 1]$, leaving the rare-earth moments at the 4a sites disordered down to T_{N2}, where additional antiferromagnetic ordering at the 4a sites sets in according to $\boldsymbol{k}_2 = [0, 0, 1]$. Such a discrete ordering at the two rare-earth sites has been observed in only a few cases, for example in Ho_3Ge_4 [16]. The fact that the distance between the 8c sites, about 6.2 Å, is much smaller than that between the 4a sites, about 8.8 Å, can explain why the ordering at the 8c sites sets in at higher temperatures (T_{N1}) than that at the 4a sites (T_{N2}). What is not yet understood is why the interaction between the 4a and 8c sites, which have a separation of only about 5.4 Å, does not lead to a coupling between the magnetic ordering at the two sites and why the moments at the 4a sites remain disordered down to a temperature (T_{N2}) where the moments at the 8c sites reach at least 95% of the saturation value.

The specific heat data on $Tb_3Pd_{20}Si_6$ and $Ce_3Pd_{20}Ge_6$ are compared in figure 1. In contrast to the λ-type C_p-anomalies at the Néel temperatures T_{N1} and T_{N2}, a small rounded C_p-anomaly is observed at T_{Q1}. The temperature dependence of the magnetic entropy [4] suggests that the quartet Γ_8 is the crystal-field ground state for all Ce^{3+} ions, and inelastic neutron scattering data [18] located the excited-state doublet Γ_7 at 46 K (8c site) and 60 K (4a site). In this work we address the determination of the magnetic structures at the two cerium sites in $Ce_3Pd_{20}Ge_6$ and present powder neutron diffraction data down to T = 0.05 K. Because the neutrons with spin 1/2 do not couple to the quadrupolar moments, the phase transition at T_{Q1} cannot be detected in our zero-field powder neutron diffraction measurements. A direct experimental observation of the quadrupolar phase transition in $Ce_3Pd_{20}Ge_6$ can be achieved by means of sound velocity measurements [5]. As shown in the inset of figure 1, a pronounced minimum near T_{Q1} is observed for the elastic constant C_{11}, which contains in part the soft elastic mode $(C_{11} - C_{12})/2$.

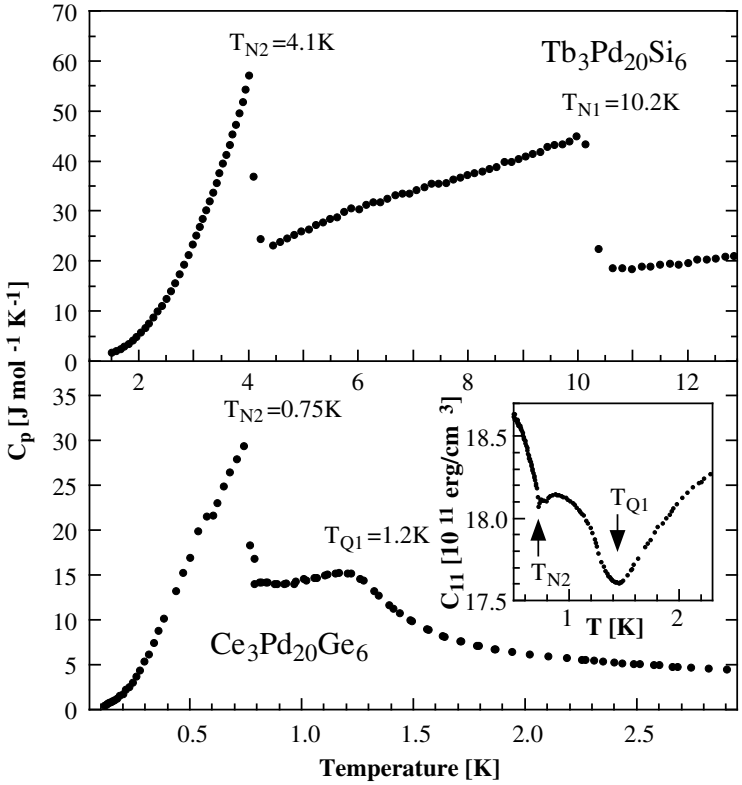

Figure 1. The temperature variation of the specific heat for polycrystalline samples of $Tb_3Pd_{20}Si_6$ [9] and $Ce_3Pd_{20}Ge_6$ [17]. Phase transitions correspond to antiferromagnetic order (T_{N1}, T_{N2}) and to quadrupolar ordering (T_{Q1}). The inset displays the minimum of the elastic constant C_{11} near T_{Q1} [5].

2. Experimental procedure

Polycrystalline $Ce_3Pd_{20}Ge_6$ material was synthesized at Tohoku University by arc melting stoichiometric amounts of the elemental constituents in an argon atmosphere and annealing for one week at 800 °C in high vacuum. Powder neutron diffraction experiments were carried out at the Institute Laue–Langevin (ILL) in Grenoble, France. The crystal structure of paramagnetic $Ce_3Pd_{20}Ge_6$ at 10 K was measured with a neutron wavelength $\lambda = 2.483$ Å on the diffractometer D1A with 25 detectors. The magnetic structures of $Ce_3Pd_{20}Ge_6$ were studied down to $T = 0.05$ K with $\lambda = 2.40$ Å on the two-axis diffractometer D20 with 1600 detectors and a high neutron flux of 3.7×10^7 neutrons s^{-1} cm^{-2} at the sample position. For the low-temperature measurement a bottom-loading $^4He/^3He$ dilution refrigerator was used and a large amount (16 g) of fine $Ce_3Pd_{20}Ge_6$ powder was filled into a special cylindrical copper container of 10 mm diameter, which allowed condensation of liquid helium into the sample voids to achieve a good thermal contact. The diffraction data were analysed using the Rietveld method for the crystal and magnetic structure refinement with the program FULLPROF [19] on the basis of the internal scattering length and magnetic form factor tables. The background was modelled by a fourth-order polynomial and the intensity profiles by the Thompson–Cox–Hastings pseudo-Voigt function [20].

3. Results and analysis

The D1A powder neutron diffraction pattern of paramagnetic $Ce_3Pd_{20}Ge_6$ at 10 K is displayed in figure 2. The observed Bragg peaks can be indexed with the expected face-centred cubic crystal structure and the impurity phase contributions are very weak. The refinement of 32 inequivalent Bragg peaks within the perfect 3–20–6 structure yielded the structural parameters given in table 1. The agreement of the fit for this $Ce_3Pd_{20}Ge_6$ sample ($\chi^2 = 4.2$, $R_{wp} = 8.1\%$) is rather poor compared to the refinement of the previously measured D1A data for $Tb_3Pd_{20}Si_6$ at 14.6 K ($\chi^2 = 2.1$, $R_{wp} = 4.4\%$ [9]). As shown in figure 2, for this $Ce_3Pd_{20}Ge_6$ sample, the observed intensities appear too strong for some Bragg peaks ((5, 1, 1), (3, 3, 3), (5, 3, 1) and (6, 4, 0), predominantly with odd indices) and too weak for other Bragg peaks ((8, 0, 0), (6, 6, 0), (8, 2, 2) and (6, 6, 2), predominantly with even indices). This is most probably due to slightly incorrect site occupation numbers for the crystallographic sites 4a, 8c, 32f, 48h and 24e, either caused by a deviation from the assumed stoichiometry or by site disorder. The D1A neutron diffraction pattern indicates the presence of some structural imperfections (site disorder and/or vacancies) in the cubic lattice of this sample, but the number of adjustable parameters in the structural model is too high for a reliable quantitative determination. It is known [21] that for $Ce_3Pd_{20}Ge_6$ the values for T_{Q1} and T_{N2} are highly sensitive to sample quality. Indeed, during our low-temperature neutron diffraction experiments, it became apparent that this $Ce_3Pd_{20}Ge_6$ sample possesses a Néel temperature $T_{N2} = 0.63$ K, which is lower than the value $T_{N2} = 0.75$ K reported in [4], and accordingly, the undetermined value for T_{Q1} may be reduced below the reported value of about 1.2 K [4]. The somewhat inferior quality of this sample is unfortunate, but not critical for an investigation of the magnetic structures of $Ce_3Pd_{20}Ge_6$.

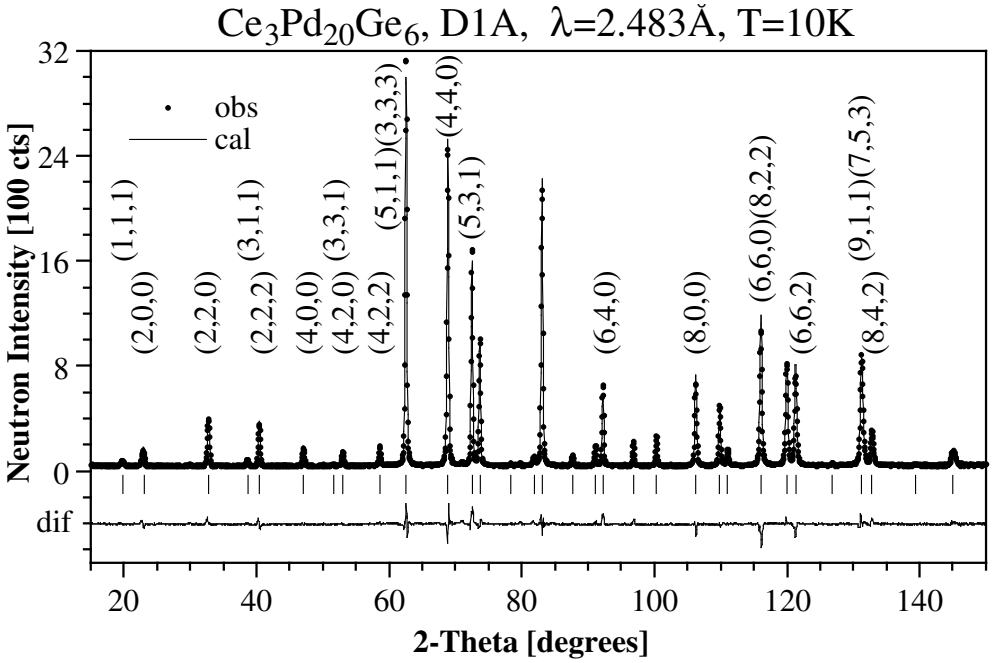

Figure 2. The D1A neutron diffraction pattern ($\lambda = 2.483$ Å) of paramagnetic $Ce_3Pd_{20}Ge_6$ at 10 K, with the results of fitting by the Rietveld method. Peak positions are indicated by vertical bars.

Table 1. Structural parameters of paramagnetic $Ce_3Pd_{20}Ge_6$ at 10 K (space group $Fm\bar{3}m$, No 225, $Z = 4$) refined from D1A powder neutron diffraction data. The fit yielded the lattice parameter $a = 12.413(5)$ Å and the agreement indices $R_{I,N} = 6.24\%$ (for integrated magnetic intensities), $R_{wp} = 8.10\%$ (for weighted intensities), $R_{exp} = 3.97\%$ (the expected value calculated from counting statistics), $\chi^2 = (R_{wp}/R_{exp})^2 = 4.17$. The Debye–Waller factor was kept fixed for all atoms at $B = 0.1$ Å^2.

Atom	Site	x/a	y/a	z/a
Ce1	4a	0	0	0
Ce2	8c	1/4	1/4	1/4
Pd1	32f	0.3834(2)	0.3834(2)	0.3834(2)
Pd2	48h	0	0.1747(2)	0.1747(2)
Ge1	24e	0.2684(2)	0	0

The D20 powder neutron diffraction data for $Ce_3Pd_{20}Ge_6$ are displayed in figure 3 as difference patterns with the data measured at $T = 0.70$ K subtracted. In these diagrams the contributions from nuclear scattering are to a good approximation eliminated, and we are left with pure magnetic neutron diffraction patterns. For 3–20–6 compounds the expected magnetic propagation vectors are $\boldsymbol{k}_1 = [1, 1, 1]$ for $T < T_{N1}$ and $\boldsymbol{k}_2 = [0, 0, 1]$ for $T < T_{N2}$. The most prominent feature of the D20 patterns shown in figure 3 is that for $Ce_3Pd_{20}Ge_6$, where T_{N1} is replaced by T_{Q1}, the antiferromagnetic Bragg peaks corresponding to $\boldsymbol{k}_1 = [1, 1, 1]$ are not observed down to the lowest measured temperature $T = 0.05$ K. For such a magnetic structure, our experiment gives a small upper limit for an ordered moment of $\mu_1(8c, \boldsymbol{k}_1 = [1, 1, 1]) < 0.13\ \mu_B$/Ce at $T = 0.05$ K, based on the experimental error of the D20 data points near the position $2\Theta = 37.6^\circ$ of the magnetic (3, 1, 1) Bragg peak. For $Ce_3Pd_{20}Ge_6$, magnetic Bragg peaks are observed for $T < T_{N2} = 0.63$ K and they can all be indexed with the propagation vector $\boldsymbol{k}_2 = [0, 0, 1]$. The temperature dependence of the integrated magnetic neutron intensity is shown in figure 4.

We now proceed to analyse the magnetic structure of $Ce_3Pd_{20}Ge_6$ below T_{N2}. The contributions to the observed magnetic Bragg peaks arising from ordered cerium moments at the 4a site (face-centred cubic sublattice) and at the 8c site (simple cubic sublattice) can be readily identified by means of the different extinction rules for nuclear Bragg peaks for the two sites [13]: a cerium moment at the 4a site, which is ordered with the antiferromagnetic propagation vector $\boldsymbol{k}_2 = [0, 0, 1]$, contributes to all observed magnetic Bragg peaks. For an ordered cerium moment at the 8c site, a propagation vector $\boldsymbol{k}_1 = [0, 0, 1]$ gives rise to magnetic Bragg peaks with only (even, even, odd) indices, whereas $\boldsymbol{k}_1 = [1, 1, 0]$ results in reflections with only (odd, odd, even) indices. Figure 5 illustrates the three possible models for magnetic structures, that are compatible with the positions of the observed magnetic Bragg peaks for $T < T_{N2}$. The cerium moments at the 4a sites are ordered with $\boldsymbol{k}_2 = [0, 0, 1]$, whereas the cerium moments at the 8c sites can be either disordered (model A), ordered with $\boldsymbol{k}_1 = [0, 0, 1]$ (model B) or ordered with $\boldsymbol{k}_1 = [1, 1, 0]$ (model C). The correct model is decided upon by comparing the intensities of the (even, even, odd) Bragg peaks, shown in the left-hand frame of figure 4, with those of the (odd, odd, even) reflections, displayed in the right-hand frame of figure 4. Systematic Rietveld refinements using all three models were performed for all D20 difference patterns of figure 3. The results obtained at $T = 0.05$ K are summarized in table 2 and a typical fit (model A, $T = 0.05$ K) is shown in figure 6. At the 4a site, we observe antiferromagnetically ordered cerium moments that are oriented perpendicular to the propagation vector $\boldsymbol{k}_2 = [0, 0, 1]$. As shown in figure 7, they grow in a second-order phase transition at T_{N2} and reach a saturation value $\mu_2(4a) = (1.1 \pm 0.1)\ \mu_B$/Ce that is reasonably large for the crystal-field ground-state quartet Γ_8. At the 8c site, down to the lowest measured

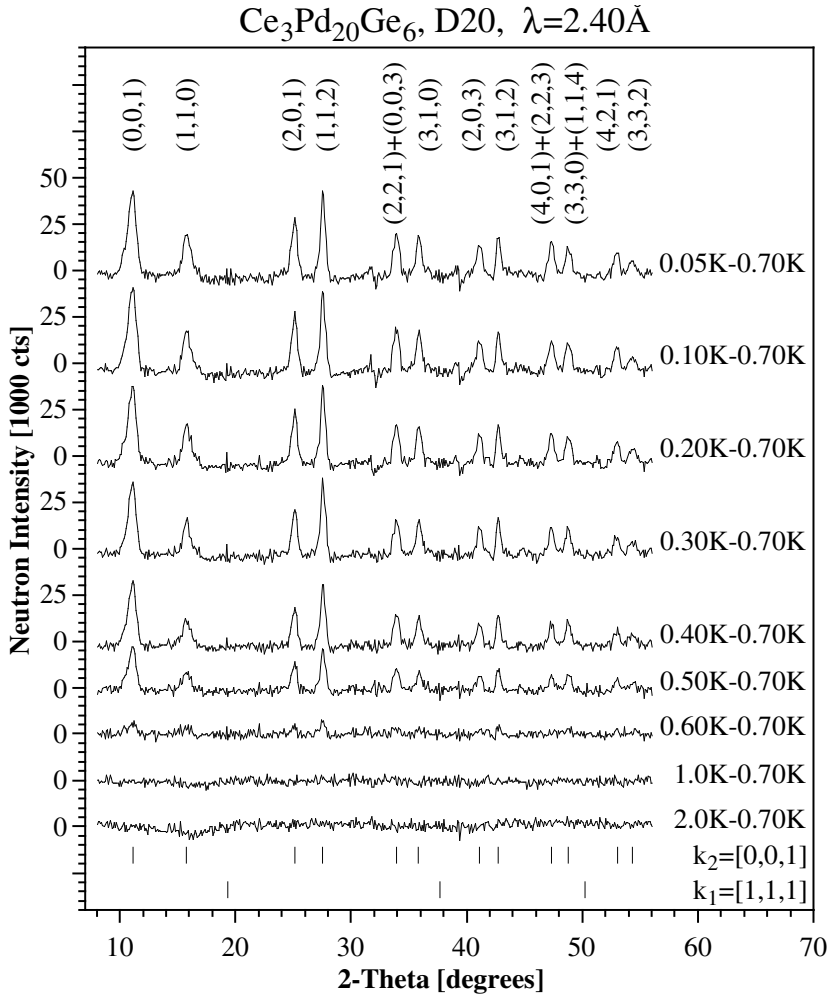

Figure 3. Difference D20 neutron diffraction patterns of $Ce_3Pd_{20}Ge_6$. The intensities have been normalized to monitor 3.0×10^8 (counting time per temperature of 110 minutes). Observed magnetic Bragg peaks can be indexed with the propagation vector $\boldsymbol{k}_2 = [0, 0, 1]$ for $T < T_{N2} = 0.63$ K. Vertical bars indicate peak positions for the propagation vectors $\boldsymbol{k}_1 = [1, 1, 1]$ (8c site) and $\boldsymbol{k}_2 = [0, 0, 1]$ (4a site).

temperature $T = 0.05$ K, a non-zero value for an ordered cerium moment (model B or C) is not significant within experimental accuracy.

4. Discussion

In CeB_6, a binary compound with a body-centred cubic crystal structure (space group $Pm\bar{3}m$, No 221), the magnetic cerium atoms are located at only one crystallographic site (1a) and are involved in both phase transitions at $T_Q = 3.3$ K and $T_N = 2.3$ K. Mainly as a result of the antiferroquadrupolar ordering at T_Q, the antiferromagnetic structure below T_N appears with a reduced cerium saturation moment, for which two groups determined controversial values of 0.3 μ_B [2] and 0.7 μ_B [22]. For $Ce_3Pd_{20}Ge_6$, a ternary compound with a face-centred cubic

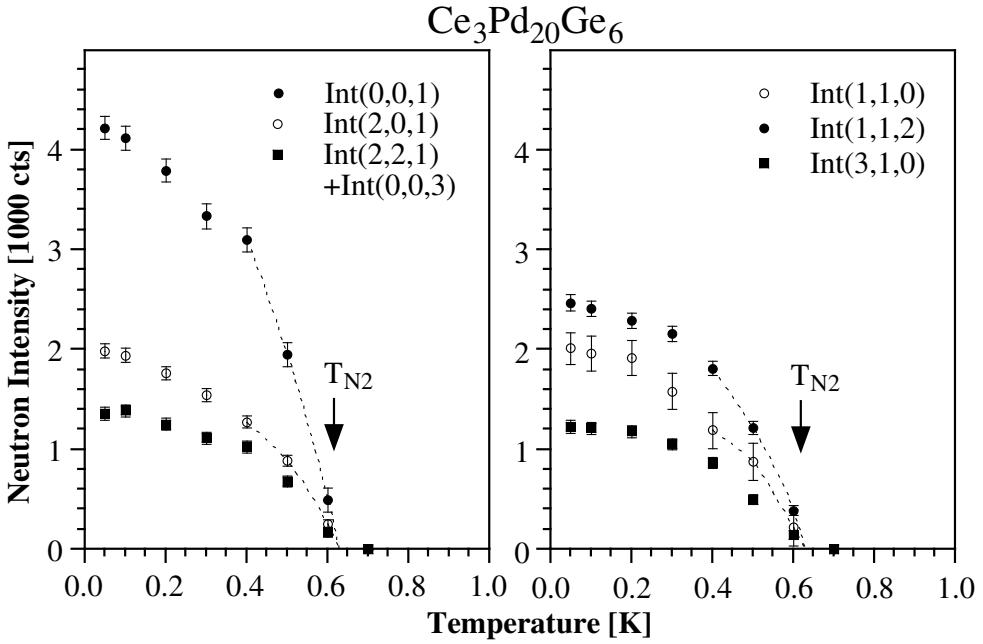

Figure 4. The temperature dependence of the integrated neutron intensity of the magnetic Bragg peaks of $Ce_3Pd_{20}Ge_6$ based on the D20 data of figure 3. The values have been carefully determined by Gaussian fits for the Bragg peaks with $2\Theta > 20^\circ$ (smaller error bars) and by integrating the intensity around the peak position for the Bragg peaks (0, 0, 1) and (1, 1, 0) with an asymmetric instrumental peak shape (larger error bars).

Table 2. Results of Rietveld refinements of the magnetic structure of $Ce_3Pd_{20}Ge_6$ at 0.05 K for the models A, B and C shown in figure 5. The number of fitting parameters was 2 (μ_2, α_2) for model A and 4 ($\mu_1, \alpha_1, \mu_2, \alpha_2$) for models B, C. α_i ($i = 1, 2$) denotes the angle between the direction of the ordered moment μ_i and the propagation vector $\boldsymbol{k}_i$. (?): these values are not significant because of the too small values for μ_1 and have therefore been fixed to $\alpha_1 = \alpha_2$.

Model	A	A	B	C
8c site:				
$\boldsymbol{k}_1$	—	—	[0, 0, 1]	[1, 1, 0]
μ_1 (μ_B/Ce)	—	—	0.0 ± 0.2	0.1 ± 0.2
α_1	—	—	90° (?)	90° (?)
4a site:				
$\boldsymbol{k}_2$	[0, 0, 1]	[0, 0, 1]	[0, 0, 1]	[0, 0, 1]
μ_2 (μ_B/Ce)	1.1 ± 0.1	1.1 ± 0.1	1.1 ± 0.1	1.1 ± 0.1
α_2	54.74°	90°	90°	90°
Agreement values:				
$R_{I,M}$ (%)	16.9	10.7	10.7	11.2
R_{wp} (%)	11.1	9.78	9.78	9.68
R_{exp} (%)	6.52	6.52	6.52	6.52
χ^2	2.90	2.25	2.25	2.20

crystal structure, the magnetic properties are complicated by the fact that the magnetic cerium atoms occupy two different crystallographic sites (8c and 4a), which in principle may both

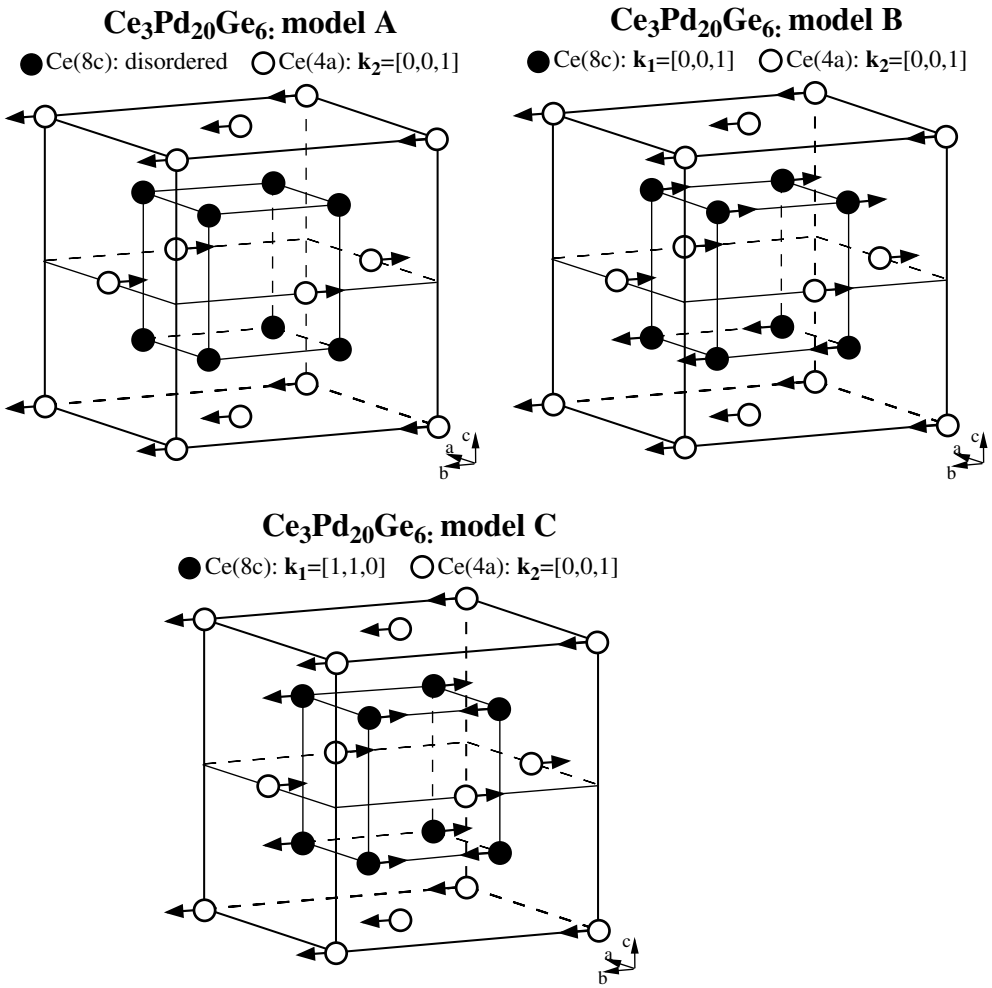

Figure 5. The three possible magnetic structures for $Ce_3Pd_{20}Ge_6$, that are compatible with the positions of the observed magnetic Bragg peaks for $T < T_{N2} = 0.63$ K.

contribute to the phase transitions at $T_{Q1} \approx 1.2$ K and $T_{N2} = 0.75$ K.

The aim of this powder neutron diffraction study was to examine the magnetic ordering at the two cerium sites in $Ce_3Pd_{20}Ge_6$. Common to all $R_3Pd_{20}X_6$ (X = Si, Ge) compounds so far investigated are the discrete magnetic ordering at the two rare-earth sites and the same magnetic propagation vectors: at the Néel temperature T_{N1} the magnetic moments at the 8c site order with a propagation vector $\boldsymbol{k}_1 = [1, 1, 1]$ and at T_{N2} the magnetic moments at the 4a site order with a propagation vector $\boldsymbol{k}_2 = [0, 0, 1]$. The analysis of our neutron diffraction data indicates that in $Ce_3Pd_{20}Ge_6$ the antiferromagnetic ordering of the cerium moments at the 4a site perfectly follows the systematic trend in 3–20–6 compounds. This includes: (a) the second-order phase transition at the Néel temperature T_{N2}; (b) the magnetic propagation vector $\boldsymbol{k}_2 = [0, 0, 1]$; and (c) the cerium saturation value which is close to the expected value for the crystal-field ground state Γ_8. The analysis of our neutron diffraction data further indicates that for $Ce_3Pd_{20}Ge_6$ the temperature dependence of the cerium moments at the 8c site is exceptional for a 3–20–6 compound. The features include the following: (a) the Néel temperature T_{N1}

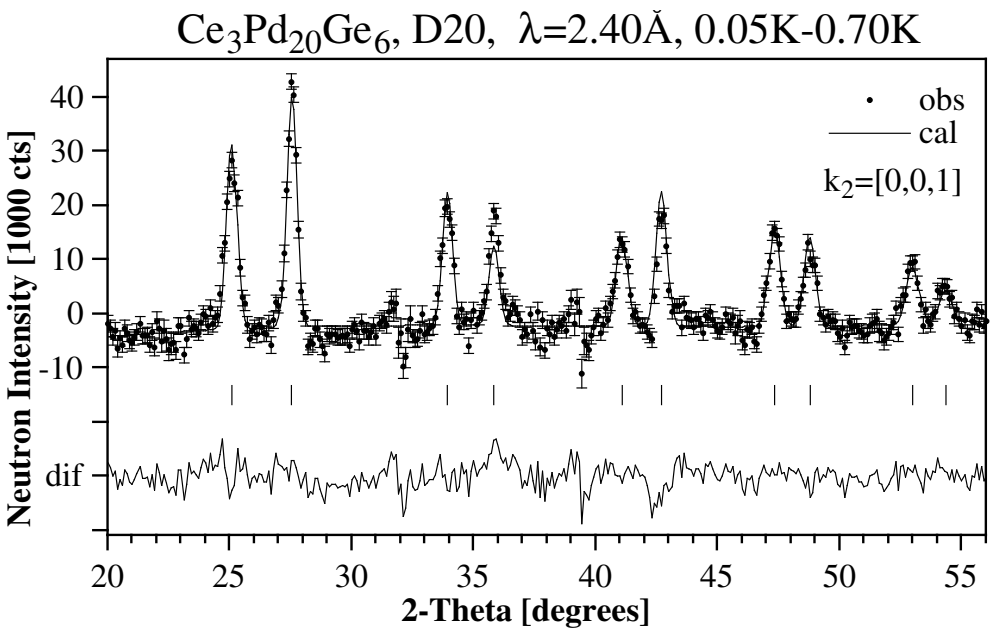

Figure 6. Rietveld refinement of the magnetic structure (model A) of $Ce_3Pd_{20}Ge_6$ at 0.05 K (obtained from the difference pattern from 0.05–0.70 K). Peak positions are indicated by vertical bars. The 2Θ region below 20°, with the Bragg peaks (0, 0, 1) and (1, 1, 0) affected by an asymmetric instrumental peak shape, was excluded during the refinement.

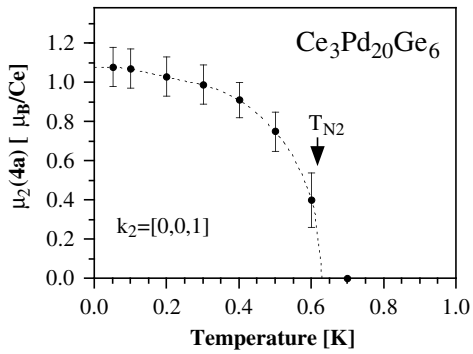

Figure 7. The temperature variation of the antiferromagnetically ordered cerium moments at the 4a site in $Ce_3Pd_{20}Ge_6$ as determined by Rietveld refinements of the D20 difference patterns shown in figure 3.

is replaced by the quadrupolar phase transition T_{Q1}; (b) the expected magnetic propagation vector $\boldsymbol{k}_1 = [1, 1, 1]$ is absent with an upper limit $\mu_1(8c) < 0.13\ \mu_B$/Ce at $T = 0.05$ K; and (c) down to the lowest measured temperature $T = 0.05$ K a possible ordered cerium moment is found to be reduced to an undetectable small value.

Including all the information mentioned in the above two paragraphs, our results provide indirect experimental evidence that in $Ce_3Pd_{20}Ge_6$ only the quadrupolar moments of cerium at the 8c site are involved in the phase transition at T_{Q1}. The ferroquadrupolar ordering at T_{Q1} generates a small distortion of the crystal lattice from cubic to tetragonal (in the case of an

order parameter O_2^0) or from cubic to orthorhombic (in the case of O_2^2). For $Ce_3Pd_{20}Ge_6$ this symmetry lowering, which is compatible with the observed propagation vector $\boldsymbol{k}_2 = [0, 0, 1]$ at the 4a site, may prevent the cerium moments at the 8c site from ordering in the preferred antiferromagnetic sequence along a cubic [1, 1, 1] direction ($\boldsymbol{k}_1 = [1, 1, 1]$). A first neutron diffraction experiment on a $Ce_3Pd_{20}Ge_6$ single crystal with $T_{N2} = 0.75$ K [23] detected very weak incommensurate magnetic Bragg peaks below about 0.45 K, which suggest that the cerium moments at the 8c site are forced to order with an incommensurate propagation vector $\boldsymbol{k} = [0, 0, 1 - \tau]$, $\tau \approx 0.06$. Despite the large sample volume and the high neutron flux, such incommensurate magnetic Bragg peaks are too weak to be detectable in our D20 powder neutron diffraction experiment.

The remaining problems to be addressed in future neutron diffraction experiments on a high-quality $Ce_3Pd_{20}Ge_6$ single crystal include: (1) the determination of the details of the incommensurate magnetic structure with strongly reduced ordered cerium moments at the 8c site; and (2) the investigation of the complex magnetic phase diagram of $Ce_3Pd_{20}Ge_6$ [24]. In particular, as has been demonstrated for UPd_3 [25], information about the quadrupolar ordering in $Ce_3Pd_{20}Ge_6$ can be obtained by measuring the field-induced magnetic structure between T_{N2} and T_{Q1}, which depends on the symmetry of the ferroquadrupolar ordering. If the future experiments confirm our prediction that only the quadrupolar moments of cerium at the 8c site are involved in the phase transition at T_{Q1}, $Ce_3Pd_{20}Ge_6$ would be the first example of a compound where the ordering of the quadrupolar moments is partly induced by the dipole ordering (below T_{N2} at the 4a sites) and partly occurs independently (below T_{Q1} at the 8c sites).

Acknowledgments

We would like to thank S Pujol for expert technical assistance in the operation of the ^{4}He/^{3}He dilution cryostat. Financial support by the Swiss National Science Foundation is gratefully acknowledged.

References

[1] Sato N, Kunii S, Oguro I, Komatsubara T and Kasuya T 1984 *J. Phys. Soc. Japan* **53** 3967
[2] Rossat-Mignod J, Burlet P, Regnault L P and Vettier C 1990 *J. Magn. Magn. Mater.* **90–91** 5
[3] Morin P 1988 *J. Magn. Magn. Mater.* **71** 151
[4] Kitagawa J, Takeda N and Ishikawa T 1996 *Phys. Rev.* B **53** 5101
[5] Suzuki O, Horino T, Nemoto Y, Goto T, Dönni A, Komatsubara T and Ishikawa M 1999 *Physica* B **259–261** 334
[6] Shiina R, Shiba H and Thalmeier P 1997 *J. Phys. Soc. Japan* **66** 1741
[7] Kitagawa J, Takeda N, Ishikawa M, Nakayama M, Kimura N and Komatsubara T 2000 *J. Phys. Soc. Japan* **69** 883
[8] Gribanov A V, Seropegin Y D and Bodak O I 1994 *J. Alloys Compounds* **204** L9
[9] Herrmannsdörfer T, Dönni A, Fischer P, Keller L, Böttger G, Gutmann M, Kitazawa H and Tang J 1999 *J. Phys.: Condens. Matter* **11** 2929
[10] Herrmannsdörfer T, Dönni A, Fischer P, Keller L and Kitazawa H 2000 *Physica* B **281–282** 167
[11] Dönni A, Keller L, Fischer P, Aoki Y, Sato H, Fauth F, Zolliker M, Komatsubara T and Endoh Y 1998 *J. Phys.: Condens. Matter* **10** 7219
[12] Kimura N, Tateiwa N, Nakayama M, Aoki H, Komatsubara T, Sakon T, Motokawa M, Koike Y and Metoki N 1999 *Physica* B **259–261** 338
[13] Dönni A, Fauth F, Fischer P, Herrmannsdörfer T, Keller L and Komatsubara T 2000 *J. Alloys Compounds* **306** 40
[14] Herrmannsdörfer T, Dönni A, Fischer P, Keller L, Clementyev E, Furrer A, Mango S, van den Brandt B and Kitazawa H 2000 *Proc. ICFE'4; J. Alloys Compounds* at press
[15] Herrmannsdörfer T 2000 unpublished results

[16] Zaharko O, Schobinger-Papamantellos P, Ritter C, Janssen Y, Brücke E, deBoer F R and Buschow K H J 1998 *J. Phys.: Condens. Matter* **10** 2881
[17] Kitagawa J, Takeda N, Ishikawa M, Yoshida T, Ishiguro A and Komatsubara T 1997 *Physica* B **230–232** 139
[18] Keller L, Dönni A, Zolliker M and Komatsubara T 1999 *Physica* B **259–261** 336
[19] Rodriguez-Carvajal J 1993 *Physica* B **192** 55
[20] Thompson P, Cox D E and Hastings J B 1987 *J. Appl. Crystallogr.* **20** 79
[21] Kitagawa J, Takeda N, Sakai F and Ishikawa M 1999 *J. Phys. Soc. Japan* **68** 3413
[22] Feyerherm R, Amato A, Gygax F N, Schenck A, Onuki Y and Sato N 1995 *J. Magn. Magn. Mater.* **140–144** 1175
[23] Dönni A, Aso N and Endoh Y 2000 unpublished results
[24] Kitagawa J, Takeda N, Ishikawa M, Yoshida T, Ishiguro A, Kimura N and Komatsubara T 1998 *Phys. Rev.* B **57** 7450
[25] McEwen K A, Steigenberger U, Clausen K N, Kulda J, Park J G and Walker M B 1998 *J. Magn. Magn. Mater.* **177–181** 37